

# Optimal tumor coverage with different beam energies by IMRT, VMAT and TOMO

## Effects on patients with proximal gastric cancer

Sheng-Fang Huang, MS<sup>a</sup>, Jang-Chun Lin, MD, PhD<sup>a,b</sup>, An-Cheng Shiau, PhD<sup>c,d,e</sup>, Yun-Chih Chen, MD<sup>a</sup>, Ming-Hsien Li, MD<sup>a</sup>, Jo-Ting Tsai, MD, PhD<sup>a,b</sup>, Wei-Hsiu Liu, MD, PhD<sup>f,g,\*</sup> 

### Abstract

To compare the effects of different photon energies on radiation planning by intensity-modulated radiotherapy (IMRT), volumetric-modulated arc therapy (VMAT) and helical tomotherapy (TOMO) for proximal gastric cancer (PGC). Network analysis with microarray procession and gene ontology were used to identify the effect of radiotherapy (RT) on PGC. Then, we retrospectively analyzed 8 PGC patients after receiving irradiation with a prescribed dose of 50.4 Gy. The Pinnacle treatment planning system (TPS, V9.8) was used to generate IMRT and VMAT plans by using 6 or 10 MV. TOMO plans were calculated on the Tomotherapy Planning Station Hi-Art Version 4.2.3 workstation (Tomotherapy Incorporated, Madison, WI, USA). PGC is associated with high DNA repair ability. TOMO plan results in higher tumor coverage and a better conformity index than IMRT and VMAT. 10-MV VMAT yields better dosimetric quality of the gradient index than 6-MV VMAT ( $P = .012$ ). TOMO was associated with a lower irradiation dose in the mean dose to the right kidney ( $P = .049$ ), left kidney and heart than 6-MV IMRT and 6-MV VMAT. 6-MV IMRT plan presented a higher dose of lung  $D_{mean}$  ( $P = .017$ ) than 10-MV IMRT. Additionally, VMAT, using a planning energy of 6 MV, was associated with a significantly higher left kidney  $D_{mean}$  ( $P = .018$ ) and  $V_{10}$  ( $P = .036$ ) than a planning energy of 10 MV. TOMO is a better RT plan not only for tumor coverage but also for sparing organs at risk. IMRT and VMAT plans with 10 MV beams are more suitable than 6 MV beams for PGC treatment.

**Abbreviations:** 3DCRT = 3-dimensional conformal RT, CCRT = concurrent chemoradiotherapy, CI = conformity index, CTV = clinical target volume, DVHs = dose-volume histograms, ECOG = Eastern Cooperative Oncology Group, FN1 = fibronectins, GE = gastroesophageal, GERD = gastroesophageal reflux disease, GI = gradient index, HI = homogeneity index, IMRT = intensity-modulated radiotherapy, MUs = machine monitor units, OAR = organs at risk, PGC = proximal gastric cancer, PTV = planning target volume, RT = radiotherapy, TOMO = tomotherapy, VMAT = volumetric-modulated arc therapy.

**Keywords:** beam energy, helical tomotherapy, intensity-modulated radiotherapy, proximal gastric cancer, volumetric-modulated arc therapy

## 1. Introduction

Gastric cancer is the fourth most common type of malignancy worldwide.<sup>[1,2]</sup> Complete surgical resection continues to be considered the most effective treatment for stomach cancer.<sup>[3]</sup>

Gastric cancer is rampant worldwide, especially in Asia, and this disease is often found in advanced stages. According to a statistical analysis based on the AJCC stage of stomach cancer, unfortunately, less than 40% of patients with locally advanced stomach cancer, including regional lymph node metastasis, will

Editor: Chao Mao.

J-TT and W-HL provided equal contribution to this work.

This work was supported by the Shuang Ho Hospital, Taipei Medical University [grant numbers 108HCP-10]. Moreover, this work was also supported by TSGH-E109225 and MOST 108-2314-B-016-022.

The authors have no relevant conflicts of interest to disclose.

The datasets generated during and/or analyzed during the current study are available from the corresponding author on reasonable request.

<sup>a</sup> Department of Radiation Oncology, Shuang Ho Hospital, <sup>b</sup> Department of Radiology, School of Medicine, College of Medicine, Taipei Medical University, <sup>c</sup> Department of Biomedical Imaging and Radiological Sciences, National Yang-Ming University, Taipei, <sup>d</sup> Department of Radiation Oncology, China Medical University Hospital, <sup>e</sup> Department of Biomedical Imaging and Radiological Science, China Medical University, Taichung, <sup>f</sup> Department of Neurological Surgery, Tri-Service General Hospital and National Defense Medical Center, No. 325, Sec. 2, Cheng-Kung Road, <sup>g</sup> Department of Surgery, School of Medicine, National Defense Medical Center, Taipei, Taiwan, ROC.

\* Correspondence: Wei-Hsiu Liu, Department of Neurological Surgery, Tri-Service General Hospital and National Defense Medical Center, No. 325, Sec. 2, Cheng-Kung Road, Taipei 11490, Taiwan (ROC), Department of Surgery, School of Medicine, National Defense Medical Center, No. 161, Sec. 6, Minquan E. Rd., Neihu Dist., Taipei 114, Taiwan (ROC) (e-mail: liubear0812bear@yahoo.com.tw).

Copyright © 2020 the Author(s). Published by Wolters Kluwer Health, Inc.

This is an open access article distributed under the terms of the Creative Commons Attribution-Non Commercial License 4.0 (CCBY-NC), where it is permissible to download, share, remix, transform, and buildup the work provided it is properly cited. The work cannot be used commercially without permission from the journal.

How to cite this article: Huang SF, Lin JC, Shiau AC, Chen YC, Li MH, Tsai JT, Liu WH. Optimal tumor coverage with different beam energies by IMRT, VMAT and TOMO: effects on patients with proximal gastric cancer. *Medicine* 2020;99:47(e23328).

Received: 24 July 2020 / Received in final form: 24 September 2020 / Accepted: 20 October 2020

<http://dx.doi.org/10.1097/MD.00000000000023328>

survive for more than 5 years. However, radiotherapy (RT) and chemotherapy have recently attracted attention as treatments for patients with advanced gastric cancers. In other words, progress in malignant therapies, including chemotherapy and modern RT, provides more therapeutic options for gastric malignancies. Multimodality therapies, such as adjuvant concurrent chemoradiotherapy (CCRT), benefit patients with intermediate stages of stomach malignancy by reducing the risk of locoregional recurrence and distant metastases after an operation.<sup>[4]</sup> A landmark randomized phase III trial, Intergroup 0116 (INT-0116), was performed to compare observation and adjuvant CCRT following R0 resection of gastric cancers or gastroesophageal (GE) junction adenocarcinoma.<sup>[5]</sup> The subsequent INT-0116 trial, which incorporated the 10-year results, revealed a strong, persistent benefit from postoperative CCRT for curatively resectable GE junction cancer and stomach malignancy, especially stage T3 (invasive) primary tumors or positive lymphadenopathies. In addition, a significant anatomic shift of stomach malignancy was noted in recent years,<sup>[6]</sup> which showed that the incidence of noncardia tumors, including those located in the fundus, body and pyloric antrum, decreased, while the incidence of cardia tumors, such as proximal gastric cancer (PGC), increased.

Contemporary RT techniques have been developed over several decades, but the application of modern radiated techniques, such as adjuvant therapy for PGC, has not yet been clarified. Regarding concerns over the surrounding normal tissues, including the heart, lung and bilateral kidneys, a comparison of sparing organs at risk (OARs) by advanced planning systems with regard to different locations of gastric cancer must be performed. RT-based techniques, such as 3-dimensional conformal RT (3DCRT), intensity-modulated radiotherapy (IMRT), volumetric-modulated arc therapy (VMAT), and helical tomotherapy (TOMO), have generally been used to treat PGC. The dosimetric performance of these techniques has also been compared.<sup>[7–11]</sup> Double-arc VMAT exhibits higher tumor coverage than IMRT and single-arc VMAT,<sup>[7]</sup> while TOMO provides higher dose conformity and homogeneity. The OARs of TOMO plans have been spared at higher doses in the bone marrow, liver, and left kidney than those of 3DCRT and VMAT plans.<sup>[8]</sup> However, to our knowledge, the photon energy of TOMO is usually different from that of VMAT or IMRT when used to treat stomach cancers. Furthermore, most studies on stomach cancer regarding RT comparisons have focused on problems associated with RT techniques. However, few studies have addressed the effect of photon beam energy on dose distribution. Many studies have evaluated the effects of dosimetric results on RT planning using different photon beam energies for cancers of the lung, pancreas, and prostate gland.<sup>[12–19]</sup> To our knowledge, this is the first study to investigate the effect of photon energy on dose distribution in RT plans for PGCs.

An interesting key point is that, in general, the photon beam used in RT planning for lung cancer treatment is 6 MV, but for gastric cancer, it is 10 MV. The TOMO plan used only the photon energy of 6 MV, and there is no other choice of photon energy because of the limitation of the RT machine. As stated in a previous study,<sup>[20]</sup> the lower beam energy (6 MV) is preferred over high beam energies (10–15 MV) in the RT planning of pulmonary tumors and adjacent normal lung tissue due to the significant loss of lateral-radiated dose equilibrium for higher energy photon beams in the air space. Any gains in RT dose uniformity across steep density gradients for higher energy beams

should be measured carefully against lateral beam degradation because of penumbra widening. A reduced scattering dose yielded by the high-energy photon beam as well as almost homogeneous dose distribution at visceral tissue is found. Therefore, RT planning in gastric cancer would use higher beam energy. However, it is unclear how to choose the photon energy for a tumor between the lung and viscera. Our study is also the first to compare the effect of photon energy in contemporary RT techniques for PGC.

We designed the following study. First, we used a large database and collected human genome array data to explain why the prognosis of PGC is different from that of noncardia gastric cancer. Then, we selected patients with PGC in whom the tumors were located in the cardia portion of the stomach. The PGC radiation fields were located near the interface between the lungs and solid tissue. This means that the target is surrounded by heterogeneous tissues. Dose distribution is highly dependent on the photon beam energy used; therefore, the effect of photon energy should be evaluated. The aims of the present study were to evaluate the effect of photon beam energies (6 and 10 MV) on the dosimetric performance of IMRT and VMAT plans for PGC on the planning target volume (PTV) and OARs. Dose-volume histograms (DVHs) were generated, and metrics, such as the homogeneity index (HI), conformity index (CI), gradient index (GI), and machine monitor units (MUs), were analyzed to compare the RT plans.

## 2. Materials and methods

### 2.1. Microarray processing, network analysis and gene ontology

We collected Affymetrix Human Genome U133A Array data from the Gene Expression Omnibus (GEO) database (accession number GSE29272). As in the cardia group, we normalized 48 samples, including twelve cardia gastric cancers (TYC0001T to TYC0012T), noncardia gastric cancers (TYB0001T to TYB0012T), and their adjacent normal tissues (TYB0001N to TYB0012N; TYC0001N to TYC0012N, respectively). Based on the difference between cancer and normal tissues, we performed heatmap and clustering analyses using ORANGE (<https://orange.biolab.si>) and Prism (<https://www.graphpad.com>). We selected significant genes ( $P$  value  $<.0625$ ,  $-\log(P$  value)  $>4$ ) from the volcano plot and applied them to STRING software (<https://string-db.org>) for network analysis and gene ontology.

### 2.2. Patient selection and simulation

The collection process of patient data followed the tenets of the Declaration of Helsinki. Our retrospective study was approved by the Institutional Review Committee at Shuang Ho Hospital, Taipei Medical University. Patients previously treated at our facility for PGC were included in our study. The therapeutic RT program was approved by the multidisciplinary gastric tumor board of Shuang Ho Hospital. The inclusion criteria were as follows: (1) Cardia tumors were diagnosed by panendoscopy; (2) The age range was 20 to 80 years; (3) The tumor was removed through an operation and proven to be gastric cancer by pathology; and (4) The Eastern Cooperative Oncology Group (ECOG) performance score was 0, 1 or 2. Tumors were staged according to the 7th edition of the AJCC using 2010 criteria. Eleven patients with gastric cancer were reviewed, but 3 patients

were excluded due to inadequate planning contours. Finally, 8 male PGC patients were included in our study. All patients were at stage T3-4 and exhibited lymph node involvement after radical total gastrectomy. Patients were immobilized using a vacuum bag in the supine position with both arms raised above their heads. Oral contrast medium was used for small bowel enhanced computed tomography (CT). CT imaging was performed using a 16-slice Brilliance Big Bore CT (Philips Medical Systems, Cleveland, OH, USA) with free breathing at a slice thickness of 5 mm, and the datasets were transferred to the treatment planning system.

### 2.3. Therapeutic target and OAR delineation

The radiation oncologist delineated the therapeutic target and surrounding critical organs according to the Radiation Therapy Oncology Group reports 50 and 62. The clinical target volume (CTV) included surgical clips postoperative imaging to define the operative tumor bed with remaining stomach and the involved lymph drainage region including perigastric, celiac, periesophageal lymphatic region.<sup>[21]</sup> The PTV was defined as a uniform 5-mm extension of the CTV to account for daily setup error and organ motion. The OARs consisted of the liver, bilateral kidneys, spinal cord, heart, lungs, and small bowel. The small bowel was delineated for 5 CT slices extending superior and inferior beyond the PTV borders. Except for the small bowel, the OARs were contoured as the entire volume, overlapping coverage with the PTV. Normal tissue was defined as the entire body excluding the PTV.

### 2.4. Dose prescription and constraints

The prescription dose to the PTV was 50.4 Gy, delivered in 28 fractions. All the plans were optimized with the objective of covering at least 97% of the PTV using 97% of the prescription dose, and the volume receiving >115% of the prescription dose was avoided. The dose constraints ( $V_x$  = volume (%) receiving  $\times$  dose (Gy) or higher) for the OARs were set as follows: mean dose ( $D_{\text{mean}}$ ) < 25 Gy for the liver;  $V_{20}$  < 33% and  $D_{\text{mean}}$  < 18 Gy for both kidneys;  $V_{30}$  < 40% and  $D_{\text{mean}}$  < 26 Gy for the heart;  $V_{20}$  < 30% and  $D_{\text{mean}}$  < 20 Gy for both lungs;  $V_{45}$  < 195 cm<sup>3</sup> for the small bowel; and maximum dose ( $D_{\text{max}}$ ) < 45 Gy for the spinal cord. According to the clinical procedure of planning optimization, a tighter dose constraint to the OARs was set during planning if a relatively low dose to the OARs was achievable.

### 2.5. Treatment planning

For 8 PGC patients who had no initial prospective IMRT, VMAT or TOMO plan, all RT plans were reprogrammed retrospectively to be able to compare optimal IMRT, VMAT and TOMO dosimeters. The treatment plans were generated using IMRT and VMAT techniques with different beam energies, including 6 or 10 MV, using the Pinnacle treatment planning system (Philips, Version 9.8.0, Fitchburg, WI, USA). The IMRT plans consisted of 6 coplanar beams at gantry angles of 300°, 340°, 20°, 60°, 100°, and 140°, and they were optimized using the direct machine parameter optimization (DMPO) algorithm with a step-and-shoot multileaf collimator delivery method. For the IMRT plans, a maximum segment number of 70, a minimum segment area of 4 cm<sup>2</sup>, and a minimum segment of 3 MUs were used during optimization.

The VMAT plans consisted of double arcs with a gantry rotation of 181°–180°–181° and were optimized using the

SmartArc planning algorithm. For the VMAT plans, the collimator angle was set to 10° to minimize the tongue-and-groove effect. A maximum delivery time of 200 s/arc and a final gantry spacing of 4° were used during optimization. Leaf motion was constrained to 0.33 cm/°. The maximum leaf velocity, gantry velocity, and variable dose rate were 2 cm/s, 6°/s and 600 MUs/min, respectively. All calculations were performed using adaptive convolution with 0.3-cm calculation grid spacing.

The parameters used for the TOMO planning system (Hi-Art Tomotherapy 4.1.2) were a pitch of 0.287, a modulation factor of 3.5 and a field width of 2.5 cm and were generated by using a TOMO system. OARs and CT planning targets were contoured in Pinnacle version 9.8 and transmitted to the TOMO system.

For each patient, 2 plans with 6 and 10 MV photon beams were created for both the IMRT and VMAT techniques, and a plan with 6 MV photon beams was created for the TOMO technique. These plans are referred to as 6-MV IMRT, 10-MV IMRT, 6-MV VMAT, 10-MV VMAT and 6-MV TOMO. All plans were clinically acceptable and followed Quantitative Analyses of Normal Tissue Effects in the Clinic (QUANTEC) guidelines. The objective of the plan was that 97% of the prescription dose cover at least 97% of the PTV with the lowest possible doses to OARs.

### 2.6. Plan evaluation

DVHs and dosimetric parameters were calculated and compared for the IMRT, VMAT and TOMO techniques. For PTV analysis, the minimum, mean, and maximum dose ( $D_{\text{min}}$ ,  $D_{\text{mean}}$ , and  $D_{\text{max}}$ , respectively) were calculated: the mean maximum dose irradiated into 2% of the PTV, and the mean minimum doses irradiated into 50% and 98% of the PTV ( $D_2$ ,  $D_{50}$ , and  $D_{98}$ ); the volume receiving 97% and 107% of the prescription dose was defined as  $V_{97}$  and  $V_{107}$ , respectively. Quality parameters of the RT plan, including the HI, CI, GI, and MUs, were compared.

The HI was calculated as:

$$HI = [(D_2 - D_{98})/D_{50}].$$

Here, a low HI value indicates homogeneous dose distributions.<sup>[8,9,22]</sup>

The CI was calculated as:

$$CI = VT_{\text{ref}}/VT \times VT_{\text{ref}}/V_{\text{ref}}.$$

Here,  $VT_{\text{ref}}$  is the volume of the PTV covered by the reference isodose line,  $VT$  is the PTV, and  $V_{\text{ref}}$  is the volume covered by the reference isodose line. The CI varies between 0 and 1, and a value close to 1 indicates high dose conformity to the PTV.<sup>[8,9,22]</sup>

The GI was calculated as:

$$GI = V_{50}/V_{100}.$$

Here,  $V_{50}$  is the volume covered by at least 50% of the prescription dose. A low GI indicates fast dose fall-off in the normal tissue and satisfactory organ sparing.<sup>[23]</sup>

For OAR analysis, dosimetric parameters, including  $D_{\text{mean}}$ ,  $D_{\text{max}}$ , and the relative volumes covered by the dose levels of interest, were investigated.

### 2.7. Statistical analysis

We retrospectively collected data from 8 patients included in this analysis. The results from all groups with different beam energies and different RT planning techniques, including 6-MV IMRT,

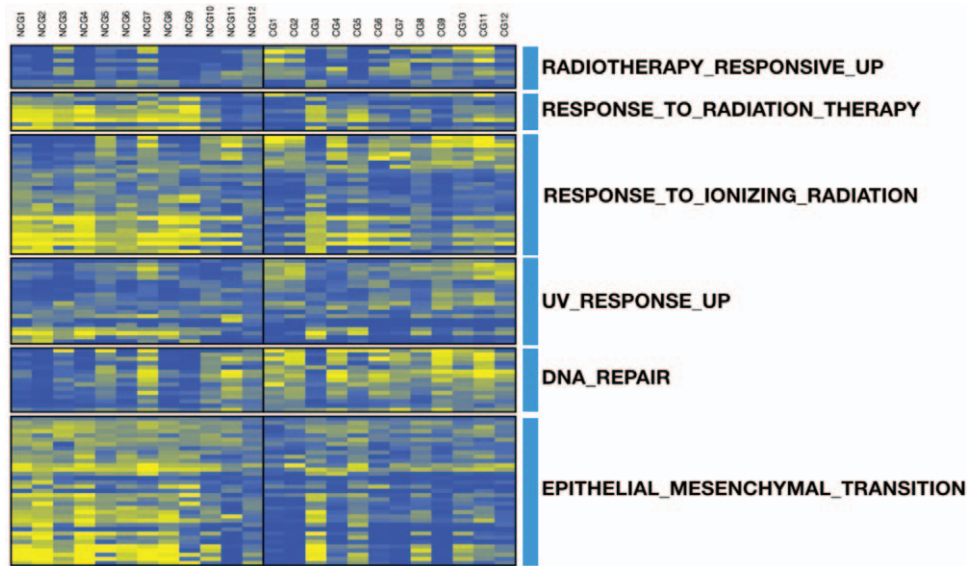


**Figure 1.** We applied microarray data to perform heatmap analysis and to explore significant genes and pathways. We collected data from Wang et al.<sup>[24]</sup> Cardia (n = 12) and non-cardia (n = 12) gastric cancer tissues were normalized to its adjacent normal tissues. We emphasized radio-resistance ability and tumor properties for observing the relationship between location and radioresistance.

10-MV IMRT, 6-MV VMAT, 10-MV VMAT and 6-MV TOMO, are presented as the mean ± standard deviation. Data were analyzed by using the Statistical Package for Social Sciences (SPSS) 20 (IBM SPSS Inc., Armonk, NY, USA). Statistically significant differences were identified by a *P* value < .05. Based on the 2-tailed Wilcoxon signed-rank test, the same beam energy with different planning groups was compared (i.e., 6-MV IMRT with 6-MV VMAT, 6-MV IMRT with 6-MV TOMO, 6-MV VMAT with 6-MV TOMO, and 10-MV IMRT with 10-MV VMAT). On the other hand, different photon energies in the same RT techniques were analyzed by Wilcoxon’s signed-rank test.

### 3. Results

#### 3.1. PGC is associated with high DNA repair ability

In general, the outcomes of gastric cancer patients are not satisfactory. Moreover, several studies have reported that cardia-type gastric cancer, PGC, is associated with worse outcomes than common gastric cancer, suggesting that PGC has the different tumor biology. To fully address these observations, we aimed to provide biological evidence to explain differences in clinical outcomes. We examined 24 patient samples from the GEO database: 12 cardia and 12 noncardia gastric cancer tissues and adjacent normal tissues.<sup>[24]</sup> These 24 samples were normalized with the Robust Multi-array Average algorithm and corrected with each adjacent normal tissue. The processed data obtained from the cardia and noncardia samples were clustered and are shown in a heatmap (Fig. 1). We identified 6 dominant phenotypes: “radiotherapy responsive upregulation”, “response to radiation therapy”, “response to ionizing radiation”, “UV response upregulation”, “DNA repair”, and “epithelial-mesenchymal transition”. Some dominant phenotypes, including “radiotherapy responsive upregulation”, “response to radiation therapy”, “response to ionizing radiation”, and “UV response upregulation”, were reduced in cardia gastric cancer, suggesting

that PGC may be insensitive to radiation. We also found that cardia gastric cancer has high DNA repair ability. We selected candidate radioresistance genes for clustering analysis. We filtered cardia-abundant genes from the candidate genes for the volcano plot analysis. Significant genes (*P* < .0625) were selected and applied to network analysis (Fig. 2). We used the STRING database (<https://string-db.org/>) to obtain functional gene association networks. Network analysis revealed that the core components were fibronectins (FN1), and PCNA (Fig. 3).

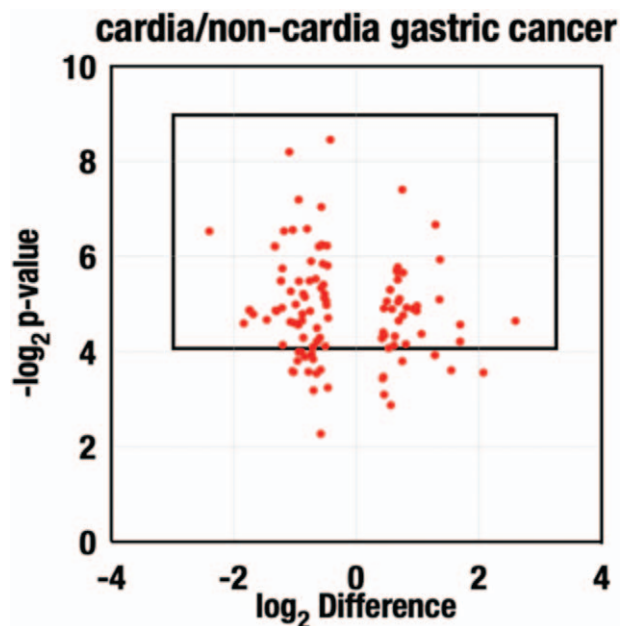


**Figure 2.** Volcano plot shows the significant genes in the comparison of the cardia and non-cardia gastric cancers. Genes with significance more than 4 (*P* value < .0625) were applied into network analysis.



**Table 2**  
**Dosimetric quality results of IMRT, VMAT and TOMO plans for PTV.**

Parameters	IMRT		VMAT		TOMO	IMRT	VMAT		6-MV		10-MV
	6-MV	10-MV	6-MV	10-MV	6-MV	6-MV vs 10-MV	6-MV vs 10-MV	IMRT vs VMAT	TOMO vs IMRT	TOMO vs VMAT	IMRT vs VMAT
	Mean ± SD					P value					
$V_{97}$ (%)	97.04 ± 0.04	97.07 ± 0.03	97.04 ± 0.04	97.08 ± 0.04	98.15 ± 0.83	NS	NS	NS	.017	.017	NS
$V_{107}$ (%)	11.56 ± 24.05	9.93 ± 19.21	1.72 ± 2.78	7.49 ± 13.84	0.3 ± 0.43	NS	NS	NS	NS	NS	NS
$D_{max}$ (Gy)	54.86 ± 1.77	54.66 ± 1.49	54.92 ± 125.94	55.36 ± 1.37	54.55 ± 0.95	NS	NS	NS	NS	NS	NS
HI	0.09 ± 0.03	0.10 ± 0.03	0.09 ± 0.09	0.10 ± 0.02	0.08 ± 0.03	NS	NS	NS	NS	NS	NS
GI	4.46 ± 0.79	4.34 ± 0.82	4.78 ± 0.90	4.38 ± 0.80	4.13 ± 0.29	NS	.012	NS	NS	.036	NS
CI	0.82 ± 0.03	0.82 ± 0.03	0.81 ± 0.06	0.82 ± 0.05	0.86 ± 0.02	NS	NS	NS	.012	.018	NS

CI = conformity index,  $D_{max}$  = maximum dose, GI = gradient index, Gy = gray, HI = homogeneity index, IMRT = intensity modulated radiation therapy, NS = nonsignificant ( $P \geq .05$ ), PTV = planning target volume, SD = standard deviation, TOMO = helical tomotherapy, VMAT = volumetric modulated radiation therapy,  $V_x$  = the volume receiving x% of prescription dose.

similar. However, plans with 10-MV VMAT were associated with a higher GI than those with 6-MV VMAT ( $P = .012$ ). Figure 4 presents the DVH of the PTV.

**3.3. Dosimetric prevention of OARs**

The 6-MV TOMO group had a lower irradiation dose in the mean dose to the right kidney ( $P = .049$ ), left kidney, heart and normal tissue, with a significant difference from 6-MV IMRT and 6-MV VMAT. However, the dose distribution to the lung was similar in the TOMO, IMRT and VMAT groups. A sample of 1 patient’s isodose curve image of 6-MV TOMO, IMRT and VMAT plans with 6 and 10-MV is shown in Figure 5. 6-MV

IMRT was associated with a lower radiation dose to the lung  $V_5$  ( $P = .025$ ) and heart  $V_{50}$  ( $P = .042$ ) than 6-MV VMAT, but 6-MV IMRT was associated with a higher radiation dose to the left kidney  $V_{20}$  ( $P = .036$ ) than 6-MV VMAT. 10-MV VMAT was associated with a lower dose to the left kidney  $D_{mean}$ ,  $V_{10}$ ,  $V_{20}$ , heart  $D_{mean}$ ,  $V_{10}$ ,  $V_{20}$  and normal tissue  $D_{mean}$ ,  $V_{25}$ ,  $V_{40}$  than 10-MV IMRT, with significant differences. Figure 4 presents a sample from 1 case of DVH in the OAR including IMRT, VMAT and TOMO.

6-MV IMRT had a higher lung  $D_{mean}$  ( $P = .017$ ) than 10-MV IMRT, and normal tissue in the 6-MV group received more irradiation than normal tissue in the 10-MV group. Furthermore, 6-MV VMAT was associated with significantly higher irradiated

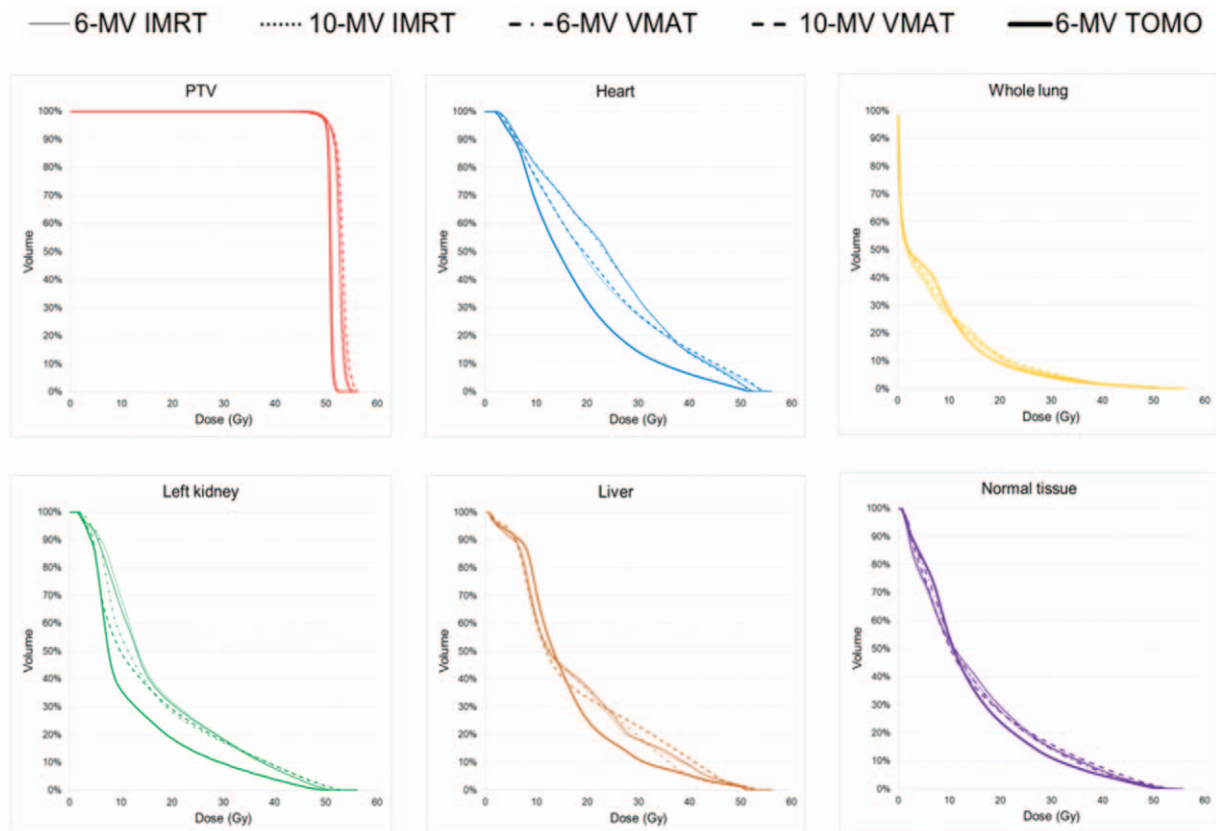
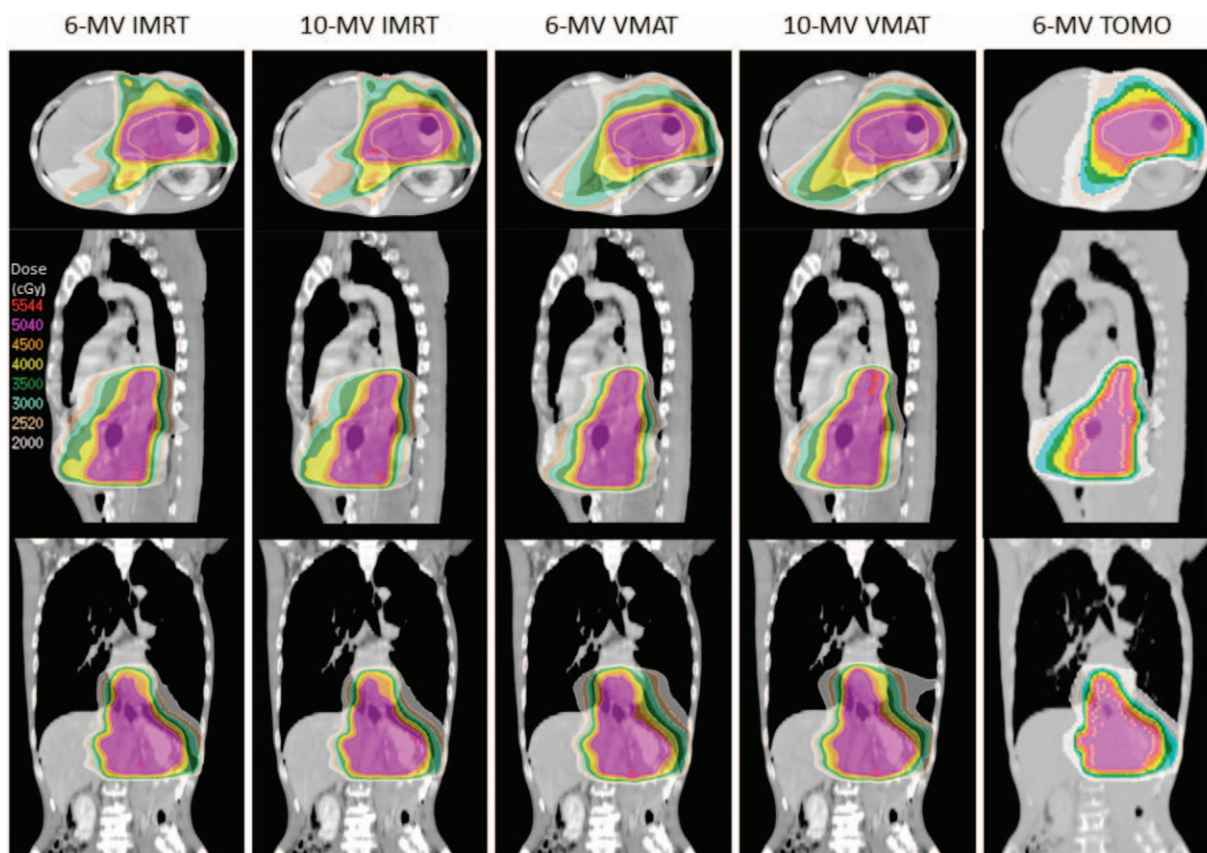


Figure 4. Representative dose volume histogram of the PTV and OARs.



**Figure 5.** Representative isodose distributions of IMRT, VMAT and TOMO plans with 6- and 10-MV photons for proximal gastric cancer in axial (above), sagittal (middle), and coronal (below) planes.

doses to the left kidney  $D_{\text{mean}}$  ( $P=.018$ ) and  $V_{10}$  ( $P=.036$ ) than 10-MV VMAT. We also found that the 10-MV VMAT group had a lower planning dose in normal tissue than the 6-MV group. A comparison of the same or different RT plans with 6- or 10-MV photon energy is presented in Table 3.

#### 4. Discussion

We identify the effect of RT on PGC through network analysis with microarray procession and gene ontology. The result finds that several genes of DNA repair is more predominant expression in PGC than noncardiac gastric cancer. FN1 bind to cell surfaces and various compounds, including collagen, fibrin, heparin, DNA, and actin. FN1 are involved in cell adhesion, cell motility, opsonization, wound healing, and maintenance of cell shape.<sup>[25]</sup> Gene ontology annotations related to this gene include sequence-specific DNA binding. PCNA helps increase the processivity of leading strand synthesis during DNA replication.<sup>[26]</sup> In response to DNA damage, this protein is ubiquitinated and is involved in the RAD6-dependent DNA repair pathway.<sup>[27]</sup> PCNA is related to protein binding, damaged DNA binding, and direct p53 effectors. High DNA repair ability was found in PGC. From the previous study, radioresistance defined that hyperactivation of DNA damage response including more DNA repair response after irradiation.<sup>[28]</sup> Therefore, PGC might be more radioresistant than noncardiac gastric cancer. Comparing different beam energies by IMRT, VMAT and TOMO could provide

insights into the development of optimal radiation skill and that might be able to overcome radioresistance.

The TOMO technique can optimize the RT plan not only for PTV coverage but also for OAR sparing, including the bilateral kidneys, heart and normal tissue. However, due to the limitation of the TOMO technique, the photon energy used in TOMO is fixed at 6 MV. Thus, after comparing IMRT with VMAT with different photon beams, it seems that IMRT and VMAT plans with 10 MV beams are more suitable than those with 6 MV beams for PGC treatment. The effect of photon energy used for VMAT and IMRT on the PTV, OARs, and normal tissue is significant. The 10-MV VMAT plans exhibited significantly lower GI values than the 6-MV VMAT plans; thus, the 10-MV VMAT plans exhibited a faster dose fall-off in the surrounding tissue than the 6-MV VMAT plans. For the left kidney, the 10-MV VMAT plans resulted in a significantly lower dose than the 6-MV VMAT plans; however, the difference in photon energies did not affect the doses to the left kidney in the IMRT plans. The mean dose to the left kidney in this study was almost the same as that reported by both Li and Wang, but the mean dose to the right kidney was lower in this study than has been previously reported.<sup>[7,10]</sup> The VMAT plans provided significantly lower  $V_{20}$  to the left kidney than did the IMRT plans. For the heart, the 10-MV VMAT plans provided a significantly lower dose than the 10-MV IMRT plans. The values of  $V_{40}$  and  $V_{50}$  for the heart in this study were lower than those reported by Wang for the IMRT and VMAT plans.<sup>[10]</sup>

**Table 3**  
The comparison of IMRT and VMAT plans with 6- and 10-MV photon beams and 6-MV TOMO for OARs.

Parameters	IMRT	VMAT		TOMO		IMRT	VMAT	6-MV	10-MV		
	6-MV	10-MV	6-MV	10-MV	6-MV	6-MV vs 10-MV	6-MV vs 10-MV	IMRT vs TOMO	TOMO vs VMAT	IMRT vs VMAT	
	Mean ± SD					P value					
Right kidney											
$D_{mean}$ (Gy)	8.08 ± 4.10	8.01 ± 4.19	8.44 ± 4.16	7.72 ± 3.93	6.52 ± 2.68	NS	NS	NS	.049	.049	NS
$V_{10}$ (%)	25.64 ± 19.28	25.39 ± 18.22	24.84 ± 17.21	22.35 ± 14.54	22.43 ± 11.99	NS	NS	NS	NS	NS	NS
$V_{20}$ (%)	11.38 ± 10.40	11.69 ± 10.42	11.60 ± 9.68	10.67 ± 9.62	4.71 ± 5.31	NS	NS	NS	NS	NS	NS
Left kidney											
$D_{mean}$ (Gy)	14.88 ± 2.58	14.85 ± 2.51	14.51 ± 1.95	14.05 ± 2.02	11.24 ± 2.75	NS	.018	NS	.012	.012	.025
$V_{10}$ (%)	54.75 ± 13.30	55.47 ± 13.58	52.68 ± 11.60	49.72 ± 11.21	38.12 ± 14.32	NS	.036	NS	.012	.012	.012
$V_{20}$ (%)	25.24 ± 6.80	24.99 ± 6.45	21.74 ± 5.07	22.25 ± 5.54	13.99 ± 7.04	NS	NS	.036	.012	.012	.036
Liver											
$D_{mean}$ (Gy)	17.67 ± 2.91	17.57 ± 2.80	18.01 ± 2.22	17.74 ± 2.35	16.25 ± 2.64	NS	NS	NS	.017	.012	NS
$V_{30}$ (%)	19.70 ± 6.91	19.49 ± 6.80	20.61 ± 5.78	20.49 ± 6.08	11.83 ± 5.64	NS	NS	NS	.012	.012	NS
Heart											
$D_{mean}$ (Gy)	17.30 ± 6.95	17.37 ± 6.98	16.68 ± 6.27	16.62 ± 6.68	14.03 ± 5.37	NS	NS	NS	.017	.012	.017
$V_{10}$ (%)	62.84 ± 23.87	63.60 ± 24.79	60.44 ± 22.42	60.03 ± 23.62	52.92 ± 25.23	NS	NS	NS	.025	.05	.017
$V_{20}$ (%)	38.66 ± 18.23	39.09 ± 18.35	35.06 ± 14.53	35.32 ± 16.10	24.47 ± 14.10	NS	NS	NS	.017	.017	.025
$V_{30}$ (%)	18.08 ± 10.33	17.99 ± 10.23	16.89 ± 7.86	16.74 ± 8.92	9.92 ± 5.68	NS	NS	NS	.012	.012	NS
$V_{40}$ (%)	6.40 ± 4.03	6.39 ± 4.07	6.52 ± 3.99	6.77 ± 4.57	3.65 ± 2.69	NS	NS	NS	.028	.012	NS
$V_{50}$ (%)	0.67 ± 0.70	0.73 ± 0.77	1.00 ± 1.28	1.27 ± 1.62	0.32 ± 0.40	NS	NS	.042	.043	.018	NS
Lung											
$D_{mean}$ (Gy)	6.42 ± 3.27	6.27 ± 3.27	6.48 ± 3.11	6.34 ± 3.26	6.23 ± 3.01	.017	NS	NS	NS	NS	NS
$V_5$ (%)	34.18 ± 16.32	33.97 ± 16.37	36.33 ± 15.80	35.38 ± 15.46	35.18 ± 17.02	NS	NS	.025	NS	NS	NS
$V_{10}$ (%)	21.93 ± 11.11	21.87 ± 11.39	22.87 ± 10.70	22.35 ± 11.40	22.67 ± 12.77	NS	NS	NS	NS	NS	NS
$V_{20}$ (%)	9.80 ± 5.99	9.45 ± 6.27	8.95 ± 5.51	8.91 ± 6.45	7.44 ± 5.97	NS	NS	NS	NS	NS	NS
$V_{30}$ (%)	3.97 ± 3.38	3.89 ± 3.44	3.79 ± 3.34	3.98 ± 3.81	3.21 ± 2.93	NS	NS	NS	NS	NS	NS
Normal tissue											
$D_{mean}$ (Gy)	15.33 ± 1.39	15.10 ± 1.38	15.74 ± 1.59	15.40 ± 1.66	13.33 ± 2.01	.025	.036	.025	.12	.12	.025
$V_{10}$ (%)	52.8 ± 3.51	52.4 ± 3.48	54.31 ± 4.41	53.27 ± 5.27	45.68 ± 8.71	.030	NS	NS	.049	.036	NS
$V_{20}$ (%)	31.74 ± 3.63	30.50 ± 3.76	31.26 ± 5.32	30.04 ± 4.74	24.90 ± 5.09	.017	.012	NS	.012	.012	NS
$V_{25}$ (%)	21.99 ± 4.23	21.26 ± 4.38	23.04 ± 4.72	22.22 ± 4.33	18.46 ± 4.21	.017	NS	.036	.017	.017	.017
$V_{40}$ (%)	6.42 ± 2.41	6.41 ± 2.45	7.05 ± 2.59	7.17 ± 2.46	7.29 ± 2.49	NS	NS	.036	NS	NS	.036

$D_{max}$  = mean dose, IMRT = intensity modulated radiation therapy, NS = nonsignificant ( $P \geq .05$ ), OARs = organs at risk, SD = standard deviation, TOMO = helical tomotherapy, VMAT = volumetric modulated radiation therapy,  $V_x$  = the volume receiving  $\geq x$  Gy.

A previous study revealed that exposure of the heart to ionizing radiation during RT for breast cancer increases the subsequent rate of ischemic heart disease, and the increase in rate is proportional to the mean dose to the heart (increased the rate of major coronary events by 7.4% per Gy, without an apparent threshold).<sup>[29]</sup> Doses to the heart were relatively less frequent in studies on RT for PGC, but studies have recommended paying attention to these doses to reduce the risk of heart disease, particularly for patients with PGC. For the lungs, the mean lung dose was <7 Gy in all plans. The 10-MV IMRT plans exhibited a significantly lower mean dose than the 6-MV IMRT plans, but the 6-MV VMAT plans exhibited a slightly higher  $V_5$  than the 6-MV IMRT plans. The risk of radiation-induced secondary lung cancer was affected mainly by the RT technique in the study of Corradini et al.<sup>[30]</sup> Although the difference between the VMAT and IMRT groups was small in this study, the lung dose should be considered during RT for PGC. For normal tissue, the 6-MV plans exhibited significantly higher doses than the 10-MV plans for both IMRT and VMAT, and the VMAT plans exhibited significantly higher doses than the IMRT plans at both 6 MV and 10 MV. These results are in agreement with the results of Pasler et al.<sup>[14]</sup> Although the doses to the normal tissue differed significantly between the 6 and 10-MV plans, distinguishing their representative lines in the DVH was difficult because the

difference was small. The mean dose to the liver in this study was lower than that reported in some studies.<sup>[7,10]</sup>

Madani demonstrated that the central location of the target may require the use of low photon energy for IMRT in patients with lung cancer. However, Weiss indicated that high photon energies should not be rejected if a dose-calculation algorithm can be used to properly correct the heterogeneity.<sup>[13]</sup> Precise optimization algorithms are necessary for resolving high-energy beams in the thorax region when the lung tissue lies in the PTV.<sup>[13]</sup> The use of photon beams with high energy for a deep tumor can provide uniform dose distribution and a low skin dose, but the target coverage may decrease because of a lack of electronic equilibrium.<sup>[12]</sup> The beam penumbra and irradiated volume increase with an increase in the lateral scatter in low-density tissue.<sup>[12]</sup> An acceptable compromise should be achieved between the penetration ability and lateral extension for the selection of suitable beam energies.<sup>[13]</sup>

Another issue is that radiation can induce secondary malignancy, and the probability is related to the volumes that received a low radiation dose.<sup>[17]</sup> High-energy photons exhibit a smaller low-dose-irradiated volume. Wiezorek and Kry<sup>[31-34]</sup> suggested that neutron contamination contributed a significant portion of the out-of-field dose equivalent when photon treatment energies were  $\geq 15$  MV, which may increase the risk of secondary malignancies.

Regardless of whether the IMRT or VMAT technique was used, 10-MV photon beams showed higher dose degradation in the surrounding normal tissue than the 6-MV beams and provided satisfactory organ sparing without sacrificing the target coverage. The VMAT plans resulted in a lower dose to the left kidney and heart but contributed more radiation to the normal tissue than the IMRT plans. In conclusion, TOMO planning optimizes the treatment plan not only for tumor coverage but also for OAR sparing. On the other hand, 10 MV photon beam planning of IMRT and VMAT is better than 6 MV beam planning for PGC treatment.

## Acknowledgments

The authors thank all the physicists and radiation oncologists from Department of Radiation Oncology of Shuang Ho Hospital, Taipei Medical University for their generous encouragement.

## Author contributions

SFH, WHL, JTT and JCL made a discussion of study design and regularly followed up the scheduled progress of the experiment. ACS and YCC performed the experimental work and analyzed the data. MHL, JCL, WHL and JTT provided biological material, and inform consent. WHL and SFH wrote the manuscript and arranged the figures in sequence. The manuscript was commented by all authors. All authors approved the final version of article.

**Conceptualization:** Wei-Hsiu Liu.

**Data curation:** Sheng-Fang Huang, Jang-Chun Lin, Yun-Chih Chen, Ming-Hsien Li.

**Formal analysis:** Sheng-Fang Huang, Jo-Ting Tsai.

**Investigation:** Jang-Chun Lin, An-Cheng Shiau.

**Resources:** An-Cheng Shiau.

**Writing – original draft:** Jang-Chun Lin.

**Writing – review & editing:** Jo-Ting Tsai, Wei-Hsiu Liu.

## References

- Miller KD, Siegel RL, Lin CC, et al. Cancer treatment and survivorship statistics, 2016. *CA Cancer J Clin* 2016;66:271–89.
- Kamangar F, Dores GM, Anderson WF. Patterns of cancer incidence, mortality, and prevalence across five continents: defining priorities to reduce cancer disparities in different geographic regions of the world. *J Clin Oncol* 2006;24:2137–50.
- Shi Y, Zhou Y. The role of surgery in the treatment of gastric cancer. *J Surg Oncol* 2010;101:687–92.
- Sandler S. Esophagogastric junction and gastric adenocarcinoma: neoadjuvant and adjuvant therapy, and future directions. *Oncology (Williston Park, NY)* 2014;28:505–12.
- Smalley SR, Benedetti JK, Haller DG, et al. Updated analysis of SWOG-directed intergroup study 0116: a phase III trial of adjuvant radiochemotherapy versus observation after curative gastric cancer resection. *J Clin Oncol* 2012;30:2327–33.
- Camargo MC, Anderson WF, King JB, et al. Divergent trends for gastric cancer incidence by anatomical subsite in US adults. *Gut* 2011;60:1644–9.
- Li Z, Zeng J, Wang Z, et al. Dosimetric comparison of intensity modulated and volumetric arc radiation therapy for gastric cancer. *Oncol Lett* 2014;8:1427–34.
- Onal C, Dolek Y, Akkus Yildirim B. Dosimetric comparison of 3-dimensional conformal radiotherapy, volumetric modulated arc therapy, and helical tomotherapy for postoperative gastric cancer patients. *Jpn J Radiol* 2018;36:30–9.
- Serarslan A, Ozbek Okumus N, Gursel B, et al. Dosimetric comparison of three different radiotherapy techniques in antrum-located stomach cancer. *Asian Pac J Cancer Prev* 2017;18:741–6.
- Wang X, Li G, Zhang Y, et al. Single-arc volumetric-modulated arc therapy (sVMAT) as adjuvant treatment for gastric cancer: dosimetric comparisons with three-dimensional conformal radiotherapy (3D-CRT) and intensity-modulated radiotherapy (IMRT). *Med Dosim* 2013;38:395–400.
- Wieland P, Dobler B, Mai S, et al. IMRT for postoperative treatment of gastric cancer: covering large target volumes in the upper abdomen: a comparison of a step-and-shoot and an arc therapy approach. *Int J Radiat Oncol Biol Phys* 2004;59:1236–44.
- Madani I, Vanderstraeten B, Bral S, et al. Comparison of 6 MV and 18 MV photons for IMRT treatment of lung cancer. *Radiother Oncol* 2007;82:63–9.
- Weiss E, Siebers JV, Keall PJ. An analysis of 6-MV versus 18-MV photon energy plans for intensity-modulated radiation therapy (IMRT) of lung cancer. *Radiother Oncol* 2007;82:55–62.
- Pasler M, Georg D, Wirtz H, et al. Effect of photon-beam energy on VMAT and IMRT treatment plan quality and dosimetric accuracy for advanced prostate cancer. *Strahlenther Onkol* 2011;187:792–8.
- Park JM, Choi CH, Ha SW, et al. The dosimetric effect of mixed-energy IMRT plans for prostate cancer. *J Appl Clin Med Phys* 2011;12:3563.
- Cai J, Yue J, McLawhorn R, et al. Dosimetric comparison of 6 MV and 15 MV single arc rapidarc to helical Tomotherapy for the treatment of pancreatic cancer. *Med Dosim* 2011;36:317–20.
- Onal C, Arslan G, Parlak C, et al. Comparison of IMRT and VMAT plans with different energy levels using Monte-Carlo algorithm for prostate cancer. *Jpn J Radiol* 2014;32:224–32.
- Onal C, Arslan G, Dolek Y, et al. Dosimetric analysis of testicular doses in prostate intensity-modulated and volumetric-modulated arc radiation therapy at different energy levels. *Med Dosim* 2016;41:310–4.
- Ost P, Speleers B, De Meerleer G, et al. Volumetric arc therapy and intensity-modulated radiotherapy for primary prostate radiotherapy with simultaneous integrated boost to intraprostatic lesion with 6 and 18 MV: a planning comparison study. *Int J Radiat Oncol Biol Phys* 2011;79:920–6.
- Wang L, Yorke E, Desobry G, et al. Dosimetric advantage of using 6 MV over 15 MV photons in conformal therapy of lung cancer: Monte Carlo studies in patient geometries. *J Appl Clin Med Phys* 2002;3:51–9.
- Hartgrink HH, van de Velde CJ. Status of extended lymph node dissection: locoregional control is the only way to survive gastric cancer. *J Surg Oncol* 2005;90:153–65.
- Zhang T, Liang ZW, Han J, et al. Double-arc volumetric modulated therapy improves dose distribution compared to static gantry IMRT and 3D conformal radiotherapy for adjuvant therapy of gastric cancer. *Radiat Oncol (London, England)* 2015;10:114.
- Li MH, Huang SF, Chang CC, et al. Variations in dosimetric distribution and plan complexity with collimator angles in hypofractionated volumetric arc radiotherapy for treating prostate cancer. *J Appl Clin Med Phys* 2018;19:93–102.
- Wang G, Hu N, Yang HH, et al. Comparison of global gene expression of gastric cardia and noncardia cancers from a high-risk population in china. *PLoS One* 2013;8:e63826.
- Sakai Y, Yamamori T, Yasui H, et al. Downregulation of the DNA repair enzyme apurinic/apyrimidinic endonuclease 1 stimulates transforming growth factor- $\beta$ 1 production and promotes actin rearrangement. *Biochem Biophys Res Commun* 2015;461:35–41.
- Boehm EM, Gildenberg MS, Washington MT. The Many Roles of PCNA in Eukaryotic DNA Replication. *Enzymes* 2016;39:231–54.
- Chatterjee N, Walker GC. Mechanisms of DNA damage, repair, and mutagenesis. *Environ Mol Mutagenesis* 2017;58:235–63.
- Bao S, Wu Q, McLendon RE, et al. Glioma stem cells promote radioresistance by preferential activation of the DNA damage response. *Nature* 2006;444:756–60.
- Darby SC, Ewertz M, McGale P, et al. Risk of ischemic heart disease in women after radiotherapy for breast cancer. *N Engl J Med* 2013;368:987–98.
- Corradini S, Ballhausen H, Weingandt H, et al. Left-sided breast cancer and risks of secondary lung cancer and ischemic heart disease: effects of modern radiotherapy techniques. *Strahlenther Onkol* 2018;194:196–205.
- Wiezorek T, Banz N, Schwedas M, et al. Dosimetric quality assurance for intensity-modulated radiotherapy feasibility study for a filmless approach. *Strahlenther Onkol* 2005;181:468–74.
- Wiezorek T, Voigt A, Metzger N, et al. Experimental determination of peripheral doses for different IMRT techniques delivered by a Siemens linear accelerator. *Strahlenther Onkol* 2008;184:73–9.
- Kry SF, Salehpour M, Followill DS, et al. Out-of-field photon and neutron dose equivalents from step-and-shoot intensity-modulated radiation therapy. *Int J Radiat Oncol Biol Phys* 2005;62:1204–16.
- Kry SF, Salehpour M, Titt U, et al. Monte Carlo study shows no significant difference in second cancer risk between 6- and 18-MV intensity-modulated radiation therapy. *Radiother Oncol* 2009;91:132–7.